Journal of Molecular Modeling (2024) 30:152
https://doi.org/10.1007/s00894-024-05930-3

ORIGINAL PAPER

Palladium(II)-catalyzed annulation of *N*-methoxy amides and arynes: computational mechanistic insights and substituents effects

Erick H. S. Alves[1] · **Daniel A. S. Oliveira**[1] · **Ataualpa A. C. Braga**[1]

Received: 29 February 2024 / Accepted: 7 April 2024 / Published online: 30 April 2024

Abstract

Context The combined use of transition metal-catalyzed C–H activation with aryne annulation reactions has emerged as an important strategy in organic synthesis. In this study, the mechanisms of the palladium(II)-catalyzed annulation reaction of *N*-methoxy amides and arynes were computationally investigated by density functional theory. The role of methoxy amide as a directing group was elucidated through the calculation of three different pathways for the C–H activation step, showing that the pathway where amide nitrogen acts as a directing group is preferable. At the reductive elimination transition state, an unstable seven-membered ring is formed preventing the lactam formation. A substituent effect study based on an NBO analysis, Hammet, and using a More O'Ferall-Jenks plot indicates that the C–H activation step proceeds via an electrophilic concerted metalation-deprotonation (eCMD) mechanism. The results show that electron-withdrawing groups increase the activation barrier and contribute to an early Pd–C bond formation and a late C–H bond breaking when compared with electron-donating substituents. Our computational results are in agreement with the experimental data provided in the literature.

Methods All calculations were performed using Gaussian 16 software. Geometry optimizations, frequency analyses at 393.15 K, and IRC calculations were conducted at the M06L/Def2-SVP level of theory. Corrected electronic energies, NBO charges, and Wiberg bond indexes were computed at the M06L/Def2-TZVP//M06L/Def2-SVP level of theory. Implicit solvent effects were considered in all calculations using the SMD model, with acetonitrile employed as the solvent.

Keywords C–H activation · Arynes · Annulation · Electrophilic concerted metalation-deprotonation · Reaction mechanism · DFT · Catalysis

Introduction

In the last decades, transition-metal-catalyzed C–H functionalization reactions have emerged as one of the most important strategies in organic synthesis [1–3].The ability to form carbon-carbon or carbon-heteroatom bonds from unfunctionalized C–H bonds enables the formation of valuable products with greater atom economy than conventional cross-coupling reactions [4, 5]. On the other hand, the use of arynes has gained significant attention due to their high reactivity and their practical and safe in situ generation through the Kobayashi method [6–8]. In this context, an emerging strategy involves the use of arynes combined with metal transition catalysts. This approach promotes C–H activation of the substrate followed by aryne annulation reactions resulting in the synthesis of valuable compounds [9–11].

In general, when substrates attached to nitrogen-containing directing groups are used in aryne annulation reactions, azacyclic products are obtained [12–19]. To the best of our knowledge, the Cheng/Tang team was the first to describe this reaction using an amide substrate leading to a ketone product and, unexpectedly, the lactam did not form. In 2022, they reported a palladium(II)-catalyzed annulation of N-methoxy amides and arynes, resulting in the synthesis of 9,10-dihydrophenanthrenone derivatives (Scheme 1) [20].

The catalytic cycle proposed by Cheng, Tang, and coworkers [20] is depicted in Fig. 1 (Path A). Interestingly, they found that palladium acetate activates both *ortho*-C–H and

✉ Ataualpa A. C. Braga
ataualpa@iq.usp.br

Erick H. S. Alves
erick_004@usp.br

Daniel A. S. Oliveira
danielarley452@usp.br

[1] Departament of Fundamental Chemistry, Institute of Chemistry, University of São Paulo, Av. Prof. Lineu Prestes, 748, São Paulo 05508-000, São Paulo, Brazil

Scheme 1 Palladium(II)-catalyzed annulation of N-methoxy amides and arynes

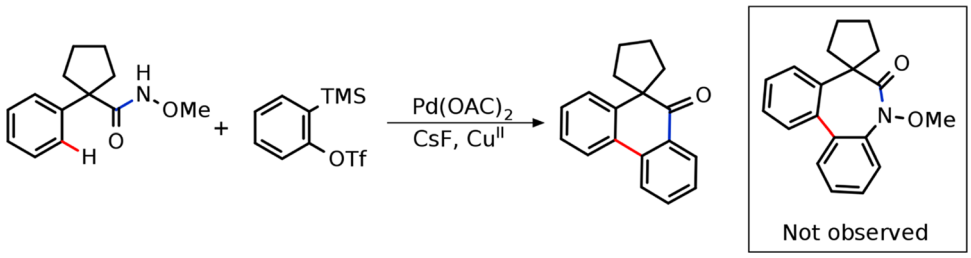

N–H bonds in the substrate to form the palladacycle **1-A**. The next step is the aryne insertion, leading to intermediate **1-B**. Instead of the eight-membered palladacycle undergoing reductive elimination to yield the lactam product, the AcOH promotes the cleavage of the Pd–N bond to give **1-C**. At this point, a nucleophilic addition to the carbonyl group is proposed to generate the cyclic intermediate **1-D**. Finally, C–N cleavage in **1-D** delivers the phenanthrenone and the alkoxyamine to regenerate the palladium catalyst. Furthermore, the authors demonstrated that copper salt promotes the oxidative decomposition of the alkoxyamine, pushing the equilibrium toward the desired ketone product [20].

Nevertheless, the lack of lactam formation in the mechanism proposed by the authors remains unexplained. To address this, Muzart [21] introduced a distinct route where the carbonyl oxygen acts as a directing group instead of the nitrogen (Fig. 1: Path B). In this alternative pathway, the C–H activation step yields the palladacycle **1-E**, which, through aryne insertion, can lead to intermediate **1-C**. According to this proposed mechanism, species **1-B** does not form, providing a possible explanation for the absence of the azacycle. Moreover, other studies in the literature also support the assignment of the carbonyl oxygen as the directing group in *ortho*-C–H activation of amides [10, 22].

Simple mechanistic understanding enables more accurate predictions for reactions involving the same or similar reactants and catalysts [23, 24]. C–H activation plays a crucial role in numerous transformations in organic synthesis, serving as the determining step for both rate- and regioselectivity in several examples [25–28]. It is known that many C–H activations catalyzed by $Pd(OAc)_2$ follow a concerted metalation-deprotonation (CMD) [29–35] mechanism, relying on the acidity of the abstracted proton [31, 32]. Controversially, in the discussed reaction [20], experimental data demonstrated that electron-withdrawing groups decrease the total yield, deviating from the expectations of a standard CMD mechanism. Competition tests favoring electron-rich substrates through a CMD mechanism are

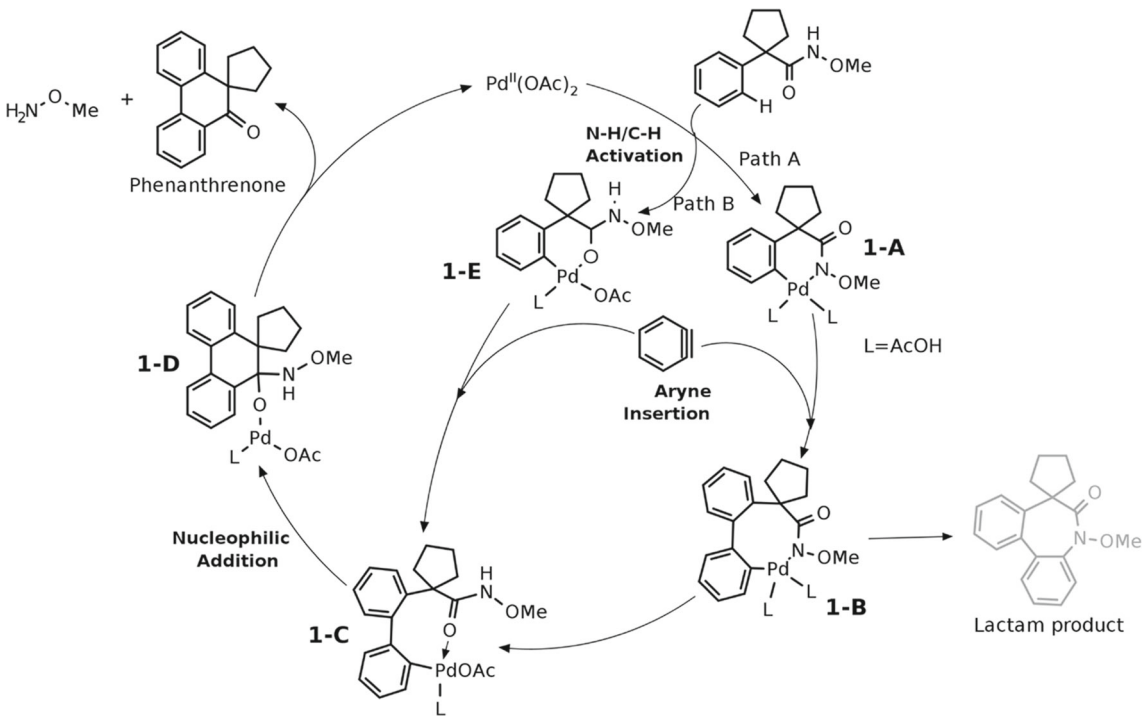

Fig. 1 The annulation reaction catalytic cycle. In Path A the amide nitrogen acts as the directing group and in Path B the C–H activation is directed by the carbonyl oxygen

known [36–45], and are better suited for a base-assisted internal electrophilic substitution type (BIES) mechanism, or an electrophilic concerted metalation-deprotonation (eCMD) mechanism [46–50].

Herein, based on the density functional theory (DFT), we investigate the mechanisms of the palladium(II)-catalyzed annulation of *N*-methoxy amides and arynes. All steps of the catalytic cycle presented in Fig. 1 have been elucidated through computational analysis. Our results contribute to clarifying the role of the methoxy amide as a directing group and offer insights into why the lactam product is not obtained in this reaction. Additionally, we conducted a substituent study on the C–H activation process to deepen our understanding of the influence of different groups on the benzene ring and the reasons for deviating from the standard CMD mechanism. Our findings suggest the presence of an eCMD mechanism instead.

Computational details

All calculations were carried out with the Gaussian 16 package [51]. Geometry optimizations were performed at the M06L/Def2-SVP level of theory [52–54]. Frequency calculations were computed at the same level of theory to obtain the thermal corrections at 393.15 K and confirm whether the structures represent transition states (TS) or minimum points on the potential energy surface. Furthermore, all transition states were validated using the intrinsic reaction coordinate (IRC) method [55]. Electronic energies were corrected at the M06L/Def2-TZVP//M06L/Def2-SVP level of theory [52–54]. The SMD [56] solvation model (solvent=acetonitrile) was applied in all calculations. The correction to bring the molecules from the gas phase at 1 atm to a solution at a concentration of 1 mol.L^{-1} was applied to the final free energies of all species. Wiberg bond indexes [57] were calculated using the natural population analysis [58] on the optimized structure of the transition states, employing the same level of theory used for computing the corrected electronic energies.

Results and discussions

Comprehensive reaction mechanism The initial step in the reaction mechanism involves the complexation of the catalyst with the substrate. Figure 2 illustrates three potential pathways for the complexation of trimeric palladium acetate $[Pd(OAc)_2]_3$ with the substrate. All pathways are endergonic due to the prior dissociation of the trimeric palladium acetate [25]. Among the three possibilities, complexation through the methoxy oxygen is the least favorable, with **int1_C** being 5.1 kcal.mol^{-1} and 6.5 kcal.mol^{-1} less stable than the **int1_A** and **int1_B**, respectively. Conversely, the complex **int1_A** resulting from the complexation of the nitrogen with the palladium can undergo N–H activation to form intermediate **int2_A**. The unfavorable deprotonation of the N–H bond is facilitated by the strong binding of the nitrogen to palladium [59], resulting in a more stable intermediate than **int1_A**. In this context, complex **int2_A** formed after the N–H activation

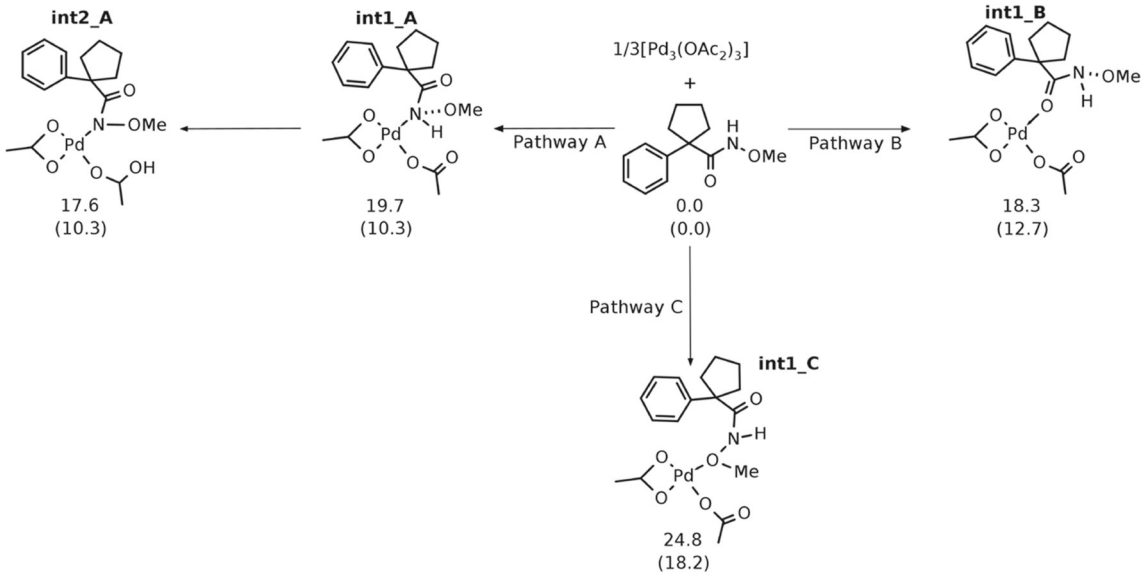

Fig. 2 Complexation of palladium acetate with the substrate. In Pathway A, the complexation occurs through nitrogen; in Pathway B, through carbonyl oxygen; and in Pathway C, through methoxy oxygen. Relative free energies (electronic energies in parentheses) with respect to separate reactants are given in kcal.mol^{-1}

is 0.7 kcal.mol^{-1} more stable than complex **int1_B**, which forms through complexation with the carbonyl oxygen.

As the free energy difference between **int2_A** and **int2_B** is not pronounced enough to decide which pathway to follow, further investigations about the C–H activation step were conducted. It became evident that relying solely on thermodynamic analysis is insufficient; therefore, it is necessary to calculate the associated transition states and their corresponding activation energies. Figure 3 depicts four transition states for C–H activation with different atoms complexed with palladium. As expected, the transition state in which the methoxy oxygen acts as a directing group has the higher energy barrier, with a value of 52.7 kcal.mol^{-1}. However, despite the small difference between **int1_B** and **int2_A** energies, an analysis of the C–H activation transition states reveals that the activation barrier of **TS2_B** is 4.4 kcal.mol^{-1} higher than the barrier to **TS2_A**, as shown in Fig. 3. Due to this high activation barrier for **TS2_B**, the pathway B, where carbonyl oxygen acts as a ligand, can be discarded. As a result, we proceed with pathway A as proposed in the literature [20]. Additionally, Fig. 3 indicates that a prior N–H activation is necessary, since **TS2_A'** (the transition state without the previous N–H activation) has a barrier 9.4 kcal.mol^{-1} higher than **TS2_A**. The transition state for N–H activation requires a barrier of 20.6 kcal.mol^{-1} concerning the separated reactants, which is only 0.9 kcal.mol^{-1} and 3.0 kcal.mol^{-1} higher than the energies of **int1_A** and **int2_A**, respectively. This result suggests the potential reversibility of the N–H activation process under the considered conditions between **int1_A** and **int2_A** due to the low forward and reverse barriers of **TS2_A** (see Fig. 4). In addition, we have also calculated **TS2_B** and **TS2_C** with the amide nitrogen deprotonated. In these cases, the energy of the deprotonated transition states is higher than that of the protonated TSs (see Fig. S1).

All the transition states presented in Fig. 3 occur via the concerted metalation-deprotonation (CMD) mechanism [32], in which the deprotonation of the C–H bond by the acetate and the formation of the Pd–C bond happen in a concerted way. While this mechanism has been extensively explored in the literature as more plausible to occur [29–35], we also investigated activation via oxidative addition and via σ-bond metathesis. The results show that both pathways have higher barriers than CMD (Fig. S1). Recognizing the importance of the preceding N–H activation step and following the pathway A illustrated in Fig. 1, the free energy profile for the Pd(II)-catalyzed annulation of *N*-methoxy amides and arynes is shown in Fig. 4. The optimized structures of the key transition states are provided in Fig. 5.

As outlined above, the initial step in the reaction mechanism is the N–H activation which occurs through the transition state **TS1** to give **int2**. An exergonic ligand exchange between acetic acid and acetonitrile takes place from **int2** to **int3**. Whenever possible, we calculated the intermediates with acetonitrile coordinating to the metal rather than acetic acid. This choice was made because acetonitrile serves as the reaction solvent and is present in much higher concentrations than the acid (see SI for more details). The subsequent C(sp^2)–H activation, denoted as **TS2**, was calculated to be 31.9 kcal.mol^{-1} above the separated reactants, with an energy barrier of 20.2 kcal.mol^{-1} relative to **int4**. From **int5** to **int6**, there is another ligand exchange, replacing the remaining acetic acid with the aryne. Subsequently, aryne insertion into **int6** gives rise to **int7** through **TS3**. Following, a new coordination of AcOH with the metal yelds **int8**. While the direct barrier of **TS3** is only 5.7 kcal.mol^{-1}, the reverse barrier is 48.8 kcal.mol^{-1}, indicating that this transformation is largely exergonic and irreversible.

At this point, two possibilities emerge: nucleophilic addition to the carbonyl group or reductive elimination (RE) to yield the lactam. Figure 6 depicts these two pathways. The black pathway represents nucleophilic addition, preceded by the nitrogen of the *N*-methoxy group's protonation by AcOH. The transition state for this proton transfer is only 0.4 kcal.mol^{-1}, indicating a rapid process. This is followed by a ligand exchange between nitrogen and carbonyl oxygen, leading to **int10** with a 1.1 kcal.mol^{-1} barrier. In the nucleophilic addition transition state (**TS5**), the palladium-bound carbon atom attacks the carbonyl group nucleophilically, with a C–C bond length of 1.99 Å.

Alternatively, the red pathway begins with an AcOH-acetonitrile ligand exchange to form **int9-RE**. Lactam formation necessitates a reductive elimination from **int9-RE**, but its energy barrier (**TS-RE**, 28.7 kcal.mol^{-1}) is higher than the nucleophilic addition barrier (26.8 kcal.mol^{-1}) relative to **int8**. This computational result favors the black pathway, explaining the ketone product instead of the azacycle.

In order to comprehend the factors influencing these reaction barriers, we conducted calculations on the reductive elimination and nucleophilic addition transition states using the substrate employed in Pimparkar and Jeganmohan's study (Scheme 2 a) [18]. The primary distinction between the substrate utilized by these authors and the one discussed in our study lies in the absence of an additional carbon atom between the benzene ring and the carbonyl group. Consequently, a more stable six-membered ring forms in their reductive elimination transition state, as opposed to the less stable seven-membered ring in our system, attributable to ring strain. Our calculations confirm this, with a significantly lower energy barrier for reductive elimination in their reaction (16.2kcal.mol^{-1}). On the other hand, the nucleophilic addition transition state involving Pimparkar's

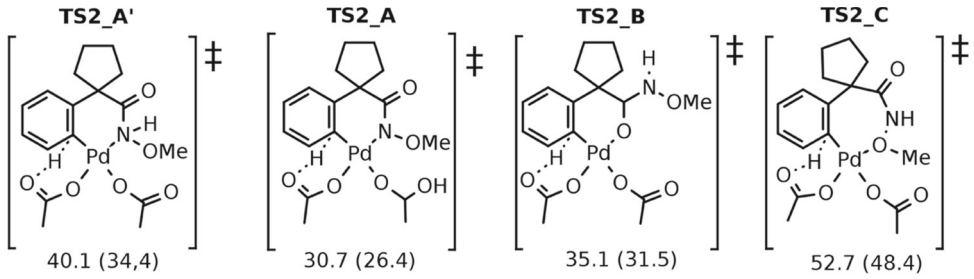

Fig. 3 C–H activation transition states with various directing groups. Relative free energies (electronic energies in parentheses) are provided in kcal.mol^{-1} relative to the separate reactants

substrate exhibits an energy barrier of 30.3 kcal.mol^{-1}, elucidating the formation of lactam in their experiment. These findings suggest that the additional carbon atom disfavors C–N bond formation while promoting C–C bond formation, ultimately preventing the lactam product in our case (Scheme 2 b).

Finally, following the nucleophilic addition pathway (black path) in Fig. 6, the nucleophilic addition transition state (**TS5**) leads to the formation of intermediate **int11**. As shown in Fig. 4, **int11** features a fully formed C–C bond. Following nitrogen protonation in **int13**, C–N cleavage occurs, resulting in the final product and regenerating the catalyst. The energy barrier for this process is only 1.3 kcal.mol^{-1} relative to **int13**. The calculated Gibbs free energy for the annulation of **N**-methoxy amides and arynes reaction is −79.8 kcal.mol^{-1}, indicating a highly exergonic reaction.

In order to verify what is the more important reaction step, the energy span model developed by Kozuch and Shaik [60] was applied to the Gibbs free energy profile. As expected, the results indicate that the C–H activation transition state (**TS2**) serves as TOF-determining transition state (TDTS), while the reactants (1/3[Pd(OAc)$_2$]$_3$ + substrate) acts as the TOF-determining intermediate (TDI). Consequently, the calculated energetic span (δE), interpreted as the apparent activation energy of the cycle, is 31.9 kcal.mol^{-1}, contributing to a TOF of $2.81 \cdot 10^{-2} h^{-1}$.

The substituents effect and the eCMD mechanism Given the significance of the C–H activation step in this reaction,

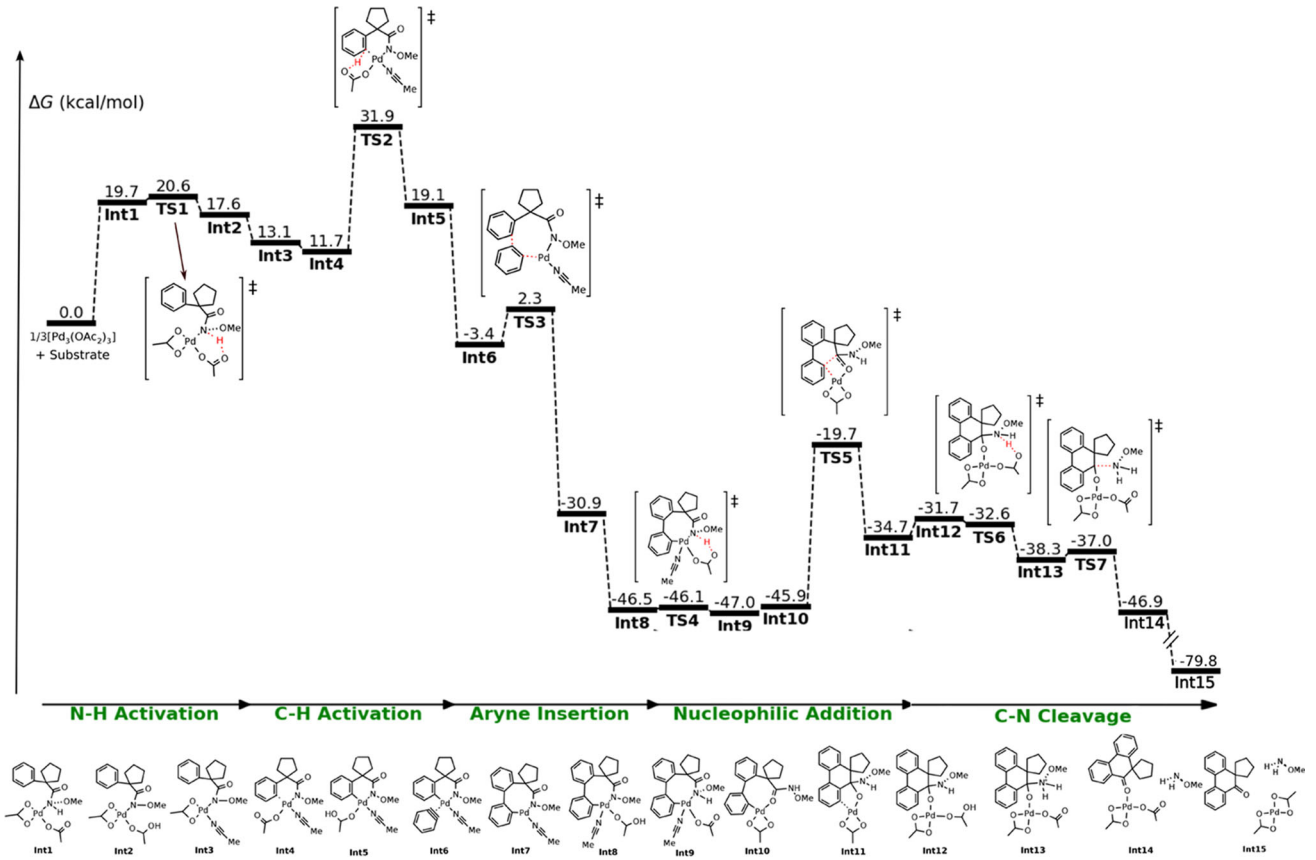

Fig. 4 Gibbs free energy profile

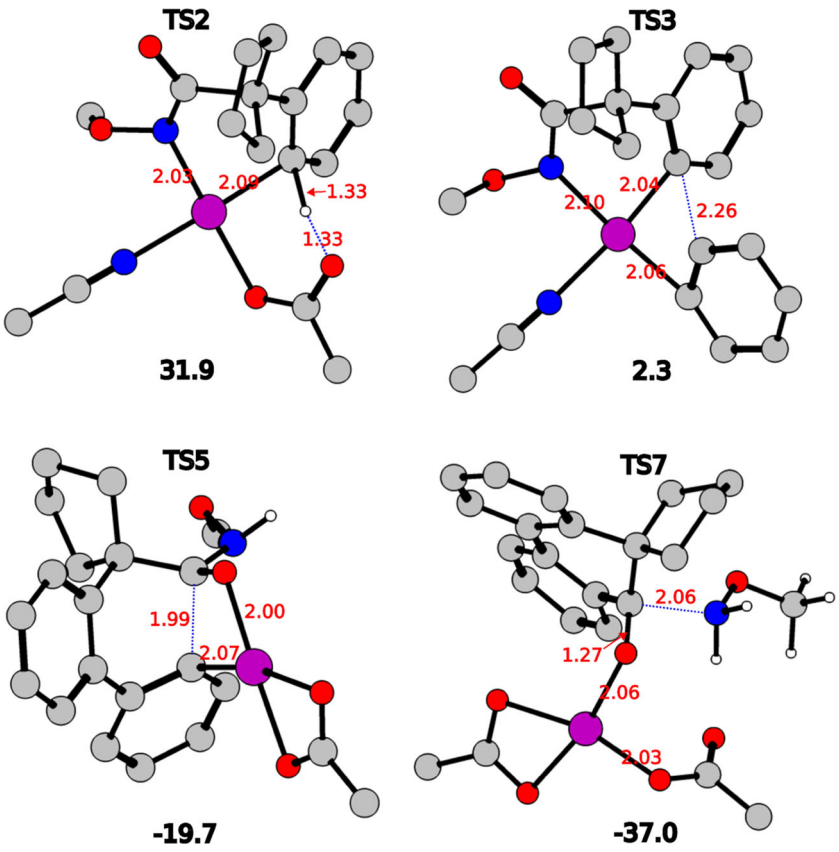

Fig. 5 Optimized transition state structures for the palladium(II)-catalyzed *N*-methoxy amide and aryne annulation reaction at the M06L/Def2-SVP level of theory. Key bond lengths are shown in Å. Relative Gibbs free energies (ΔG) for the transition states are given at the M06L/Def2-TZVP//M06L/Def2-SVP level of theory in kcal.mol^{-1}

we examine the impact of various substituents on the aromatic ring, focusing on how these changes reflect in the mechanism of interest. As discussed earlier, the experimental data deviates from the standard CMD mechanism since electron-withdrawing groups decrease the reaction yield. In this context, the computational results align with the

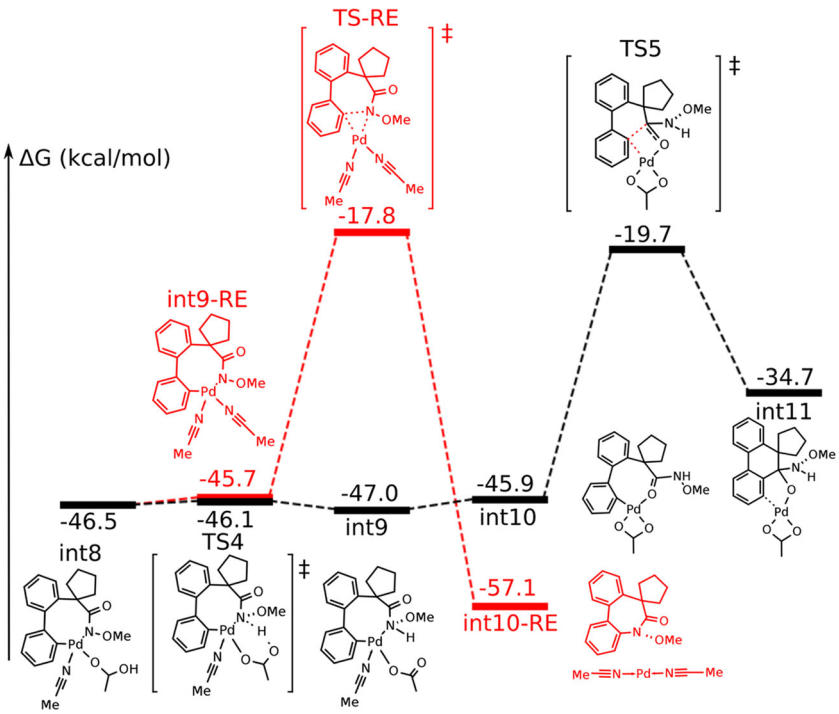

Fig. 6 Relative Gibbs free energy profiles (in kcal.mol^{-1}) for the nucleophilic addition (black path) versus reductive elimination (red path) processes

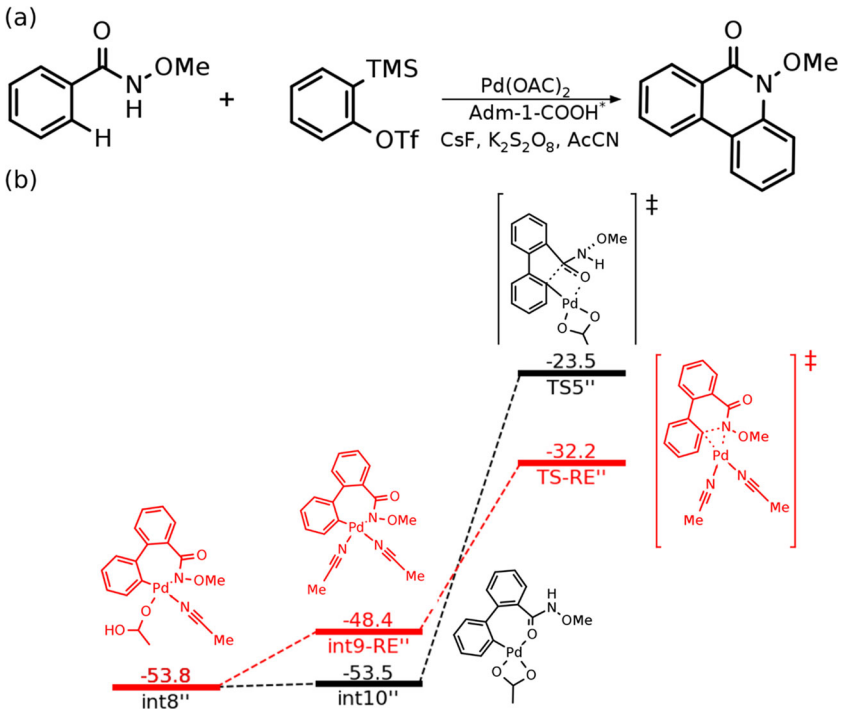

Scheme 2 (a) Reaction developed by Pimparkar/Jeganmohan Team [18]. *1-adamantanecarboxylic acid. (b) Reductive elimination and nucleophilic addition transition states to the substrate employed in the Pimparkar and Jeganmohan's study

experimental data, revealing a consistent trend. A linear relationship between the sigma constants and the calculated rate for a substituted aromatic ring in comparison to the non-substituted ring during the **TS2** step is observed (Fig. 7). The obtained slope ($\rho = -2.20$) indicates a moderate increase in positive charge on the aromatic system during the reaction.

Similar results have been reported for other concerted, base-assisted C–H cleavage reactions, which represent exceptions to the rules [61–63]. This reaction, following a S_EAr reactivity trend, explores a different region of the continuum of C–H activation mechanisms proposed by Gorelsky, Fagnou, and Lapointe [64]. This continuum accounts for

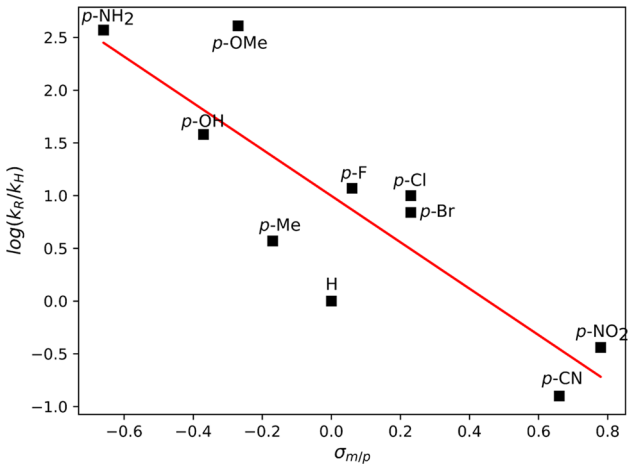

Fig. 7 Hammett analysis of substituted *N*-methoxy amides during C–H activation. Activation energies correspond to TS2

exceptions to the "classic" CMD mechanism, including S_EAr stepwise-type mechanisms.

Substituent studies guided by other computational tools suggest a base-assisted internal electrophilic substitution type (BIES), recently abbreviated as an electrophilic CMD (eCMD) mechanism that falls toward the S_EAr pole. This mechanism is characterized by an advance in metal-carbon bond formation prior to carbon-hydrogen bond cleavage [47]. Reactions that demonstrate this behavior, although tending toward arenium ion formation, conserve aromaticity.

In order to unravel the tendencies of bond breaking/forming, Wiberg bond orders derived from the C–H activation transition states were employed to construct a More O'Ferrall-Jenks plot (Fig. 8) [65, 66]. In the lower regime lies a CMD mechanism, which favors acidic protons due to the better stabilization of a negative charge accumulated on the substrate. The upper side contains an eCMD mechanism, benefiting electron-rich substrates.

As depicted in Fig. 8, all data collected in the substituent effect study fall within the range of the eCMD mechanism. The More O'Ferrall-Jenks analysis indicates that substitutions have a limited impact on the C–H bond breaking, as the C–H Wiberg bond index varies between 0.41 and 0.44. In contrast, the substituents have a more pronounced effect on the Pd–C Wiberg bond index (0.44−0.57), where electron-withdrawing substituents favor early Pd–C bond formation, while electron-donating groups favor late Pd–C bond formation.

The crucial point is that any of the substrates significantly changes the nature of the activation, as observed in other works in the literature [46–50]. Additionally, a NBO analy-

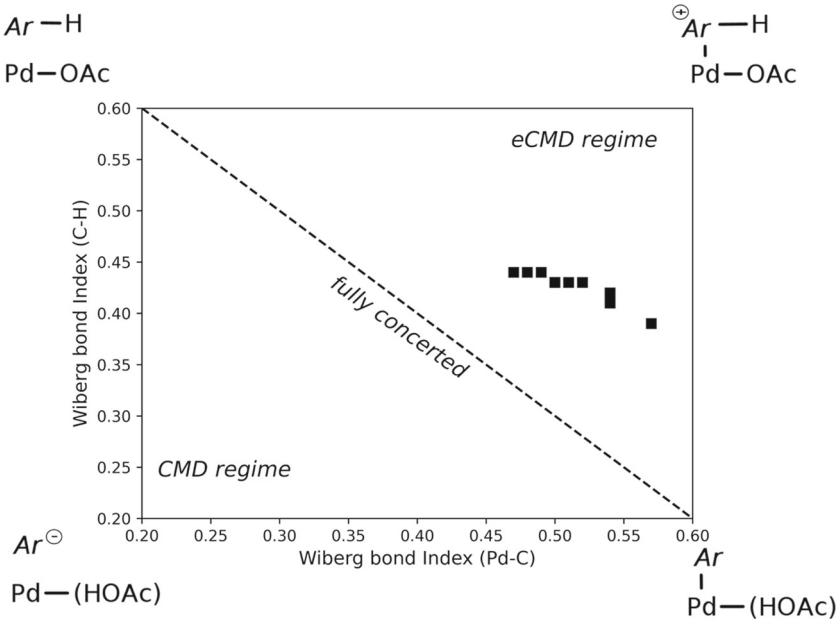

Fig. 8 More O'Ferrall-Jenks plot for C–H activation transition state with various substituents groups. See Table S1 for calculated Wiberg bond indexes for each substituent group

sis was conducted to check the built charge on the aromatic ring and on the catalyst during the transition state (Fig. 9). The analysis revealed that electron-donating groups stabilize the transition state due to their capability to transfer charge from the aromatic system to the metal. In contrast, electron-withdrawing groups destabilize the transition state by dispersing charge throughout the whole structure.

It is important to mention that, while the formation of the Pd–C bond plays a pivotal role in the reaction, the significance of C–H bond cleavage is still maintained. This is highlighted by the calculated deuterated kinetic isotope effect (KIE) of 3.81, which signifies a primary KIE in the concerted C–H activation and Pd–C bond formation mechanism. The value falls within the common range for both CMD and eCMD mechanisms [47].

Conclusions

The mechanisms for the palladium(II)-catalyzed annulation of *N*-methoxy amides and arynes were studied by means of density functional theory. The results indicate that the

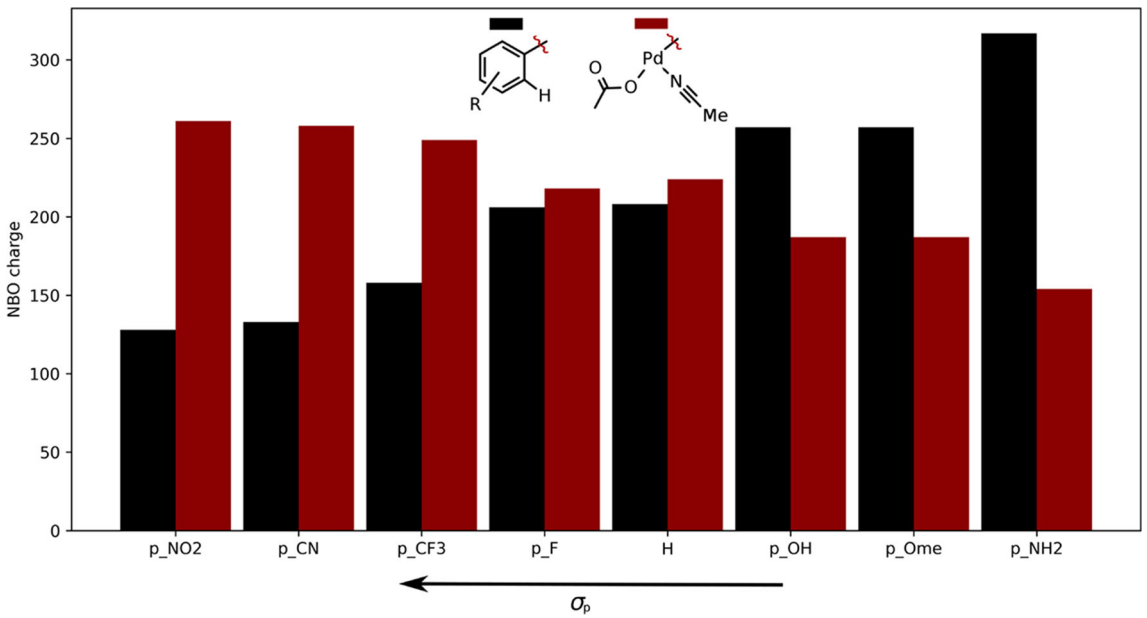

Fig. 9 NBO analysis for the C–H activation transition state with different substituents groups

amide nitrogen serves as a better-directing group than the carbonyl oxygen and methoxy oxygen. Therefore, the reaction mechanism is suggested to proceed through Path A (Fig. 1). In contrast to reactions involving nitrogen-containing substrates, the desired lactam product does not form. This outcome is attributed to the higher barrier required for reductive elimination to form the C–N bond compared to the nucleophilic addition transition state (**TS5**). The results further suggest that reductive elimination is hindered by the formation of an unstable seven-membered ring in the transition state, whereas reductive elimination leading to a six-membered lactam occurs with a more accessible barrier.

Additionally, an energy span model analysis revealed that the C–H activation transition state (**TS**) acts as the TOF-determining transition state (TDTS). Consequently, a substituent effect study was conducted in this step. Analyses based on NBO, Hammet, and More O'Ferrall-Jenks methodologies suggest that the C–H activation step proceeds through an electrophilic concerted metalation-deprotonation mechanism (eCMD). Computational data indicates that electron-withdrawing groups increase the transition state barriers, aligning with experimental data that demonstrate lower yields for electron-poor substrates compared to those containing electron-donating groups.

Supplementary Information The online version contains supplementary material available at https://doi.org/10.1007/s00894-024-05930-3.

Acknowledgements The authors acknowledge the Superintendência de Tecnologia da Informação from University of São Paulo (STI-USP), CNPq, CAPES and the São Paulo Research Foundation (FAPESP).

Author contribution Erick H. S. Alves: conceptualization, methodology, performed computations, formal analysis, writing—original draft; Daniel A. S. Oliveira: conceptualization, methodology, performed computations, formal analysis, writing—original draft; Ataualpa A. C. Braga: conceptualization, methodology, formal analysis, supervision, writing-review and edition.

Funding A.A.C.B. received financial support from São Paulo Research Foundation (FAPESP) (Grant #2015/01491-3), the Conselho Nacional de Desenvolvimento Científico e Tecnológico (CNPq) of Brazil (Grants 312550/2020-0 and 313720/2023-1), and Coordenação de Aperfeiçoamento de Pessoal de Nível Superior - Brasil (CAPES) that partially supported this work (Finance Code 001). E.H.S.A. received financial support from FAPESP (Grant #2022/16623-6). D.A.S.O. received financial support from FAPESP (Grant #2022/01685-6) and CNPq (Grant #162366/2021-3).

Data availability The inputs and outputs files of the calculations presented in the article are available in the ioChem-BD repository (https://doi.org/10.19061/iochem-bd-6-343). Additional data is provided in the supplementary information.

Declarations

Conflict of interest The authors declare no competing interests.

References

1. Rogge T, Kaplaneris N, Chatani N, Kim J, Chang S, Punji B, Schafer LL, Musaev DG, Wencel-Delord J, Roberts CA, Sarpong R, Wilson ZE, Brimble MA, Johansson MJ, Ackermann L (2021) C-H activation. Nat Rev Methods Primers 1(1):1–31. https://doi.org/10.1038/s43586-021-00041-2
2. Sinha SK, Guin S, Maiti S, Biswas JP, Porey S, Maiti D (2022) Toolbox for distal C-H bond functionalizations in organic molecules. Chem Rev 122(6):5682–5841. https://doi.org/10.1021/acs.chemrev.1c00220
3. Shang W, Sun H, Chen W, Liu J (2023) Diversification of pharmaceutical molecules via late-stage C(sp2)-H functionalization. Green Synth Catal 4(2):104–123. https://doi.org/10.1016/j.gresc.2022.12.007
4. Dalton T, Faber T, Glorius F (2021) C-H activation: toward sustainability and applications. ACS Cent Sci 7(2):245–261. https://doi.org/10.1021/acscentsci.0c01413
5. Carvalho RL, Dias GG, Pereira CL, Ghosh P, Maiti D, Silva Júnior ENd (2021) A catalysis guide focusing on c-h activation processes. J Braz Chem Soc 32:917–952. https://doi.org/10.21577/0103-5053.20210025
6. Bhunia A, Yetra SR, Biju AT (2012) Recent advances in transition-metal-free carbon-carbon and carbon-heteroatom bond-forming reactions using arynes. Chem Soc Rev 41(8):3140–3152. https://doi.org/10.1039/C2CS15310F
7. Shi J, Li L, Li Y (2021) o-Silylaryl triflates: a journey of Kobayashi aryne precursors. Chem Rev 121(7):3892–4044. https://doi.org/10.1021/acs.chemrev.0c01011
8. Takikawa H, Nishii A, Sakai T, Suzuki K (2018) Aryne-based strategy in the total synthesis of naturally occurring polycyclic compounds. Chem Soc Rev 47(21):8030–8056. https://doi.org/10.1039/C8CS00350E
9. Neog K, Borah A, Gogoi P (2016) Palladium(II)-catalyzed C-H bond activation/C-C and C-O bond formation reaction cascade: direct synthesis of coumestans. J Org Chem 81(23):11971–11977. https://doi.org/10.1021/acs.joc.6b01966
10. Li S, Liu L, Wang R, Yang Y, Li J, Wei J (2020) Palladium-catalyzed oxidative annulation of sulfoximines and arynes by C-H functionalization as an approach to dibenzothiazines. Org Lett 22(19):7470–7474. https://doi.org/10.1021/acs.orglett.0c02615
11. Yao T, He D (2017) Palladium-catalyzed domino heck/aryne carbopalladation/C-H functionalization: synthesis of heterocycle-fused 9,10-dihydrophenanthrenes. Org Lett 19(4):842–845. https://doi.org/10.1021/acs.orglett.6b03833
12. Rogness DC, Markina NA, Waldo JP, Larock RC (2012) Synthesis of pyrido[1,2-a]indole malonates and amines through aryne annulation. J Org Chem 77(6):2743–2755. https://doi.org/10.1021/jo2025543
13. Feng M, Tang B, Xu HX, Jiang X (2016) Collective synthesis of phenanthridinone through C-H activation involving a Pd-catalyzed aryne multicomponent reaction. Org Lett 18(17):4352–4355. https://doi.org/10.1021/acs.orglett.6b02109
14. Zhao J, Li H, Li P, Wang L (2019) Annulation of benzamides with arynes using palladium with photoredox dual catalysis. J Org Chem 84(14):9007–9016. https://doi.org/10.1021/acs.joc.9b00893
15. Peng X, Wang W, Jiang C, Sun D, Xu Z, Tung CH (2014) Strain-promoted oxidative annulation of arynes and cyclooctynes with benzamides: palladium-catalyzed C-H/N-H activation for the synthesis of N-heterocycles. Org Lett 16(20):5354–5357. https://doi.org/10.1021/ol5025426
16. Feng S, Li S, Li J, Wei J (2019) Palladium-catalyzed annulation of N-alkoxy benzsulfonamides with arynes by C-H functionalization: access to dibenzosultams. Org Chem Front 6(4):517–522. https://doi.org/10.1039/C8QO01311J

17. Tang CY, Wu XY, Sha F, Zhang F, Li H (2014) Pd-catalyzed assembly of phenanthridines from aryl ketone O-acetyloximes and arynes through C-H bond activation. Tetrahedron Lett 55(5):1036–1039. https://doi.org/10.1016/j.tetlet.2013.12.075
18. Pimparkar S, Jeganmohan M (2014) Palladium-catalyzed cyclization of benzamides with arynes: application to the synthesis of phenaglydon and N-methylcrinasiadine. Chem Commun 50(81):12116–12119. https://doi.org/10.1039/C4CC05252H
19. Asamdi M, Chauhan PM, Patel JJ, Chikhalia KH (2019) Palladium catalyzed annulation of benzylamines and arynes via C-H activation to construct 5,6-dihydrophenanthridine derivatives. Tetrahedron 75(25):3485–3494. https://doi.org/10.1016/j.tet.2019.05.011
20. Cheng XF, Yu T, Liu Y, Wang N, Chen Z, Zhang GL, Tong L, Tang B (2022) Palladium(II)-catalyzed C(sp2)-H bond activation/C-N bond cleavage annulation of N-methoxy amides and arynes. Org Lett 24(11):2087–2092. https://doi.org/10.1021/acs.orglett.2c00161
21. Muzart J (2022) Cross-dehydrogenative annelation of arynes with C(sp2)-H/N-H or C(sp2)-H/O-H frameworks under Pd or Cu catalysis. Tetrahedron 126:133063. https://doi.org/10.1016/j.tet.2022.133063
22. Jaiswal Y, Kumar Y, Kumar A (2018) Palladium-catalyzed regioselective C-H alkenylation of arylacetamides via distal weakly coordinating primary amides as directing groups. J Org Chem 83(3):1223–1231. https://doi.org/10.1021/acs.joc.7b02618
23. Yang YF, Hong X, Yu JQ, Houk KN (2017) Experimental-computational synergy for selective Pd(II)-catalyzed C-H activation of aryl and alkyl groups. Acc Chem Res 50(11):2853–2860. https://doi.org/10.1021/acs.accounts.7b00440
24. da Silva VHM, Oliveira CC, Correia CRD, Braga AAC (2020) Heck arylation of acyclic olefins employing arenediazonium salts and chiral N, N ligands: new mechanistic insights from quantum-chemical calculations. Theor Chem Acc 139(4):77. https://doi.org/10.1007/s00214-020-02588-x
25. Yang YF, Cheng GJ, Liu P, Leow D, Sun TY, Chen P, Zhang X, Yu JQ, Wu YD, Houk KN (2014) Palladium-catalyzed meta-selective C-H bond activation with a nitrile-containing template: computational study on mechanism and origins of selectivity. J Am Chem Soc 136(1):344–355. https://doi.org/10.1021/ja410485g
26. Dutta U, Modak A, Bhaskararao B, Bera M, Bag S, Mondal A, Lupton DW, Sunoj RB, Maiti D (2017) Catalytic arene meta-C-H functionalization exploiting a quinoline-based template. ACS Catal 7(5):3162–3168. https://doi.org/10.1021/acscatal.7b00247
27. Musaev DG, Kaledin A, Shi BF, Yu JQ (2012) Key mechanistic features of enantioselective C-H bond activation reactions catalyzed by [(chiral mono-N-protected amino acid)-Pd(II)] complexes. J Am Chem Soc 134(3):1690–1698. https://doi.org/10.1021/ja208661v
28. Yao QJ, Xie PP, Wu YJ, Feng YL, Teng MY, Hong X, Shi BF (2020) Enantioselective synthesis of atropisomeric anilides via Pd(II)-catalyzed asymmetric C-H olefination. J Am Chem Soc 142(42):18266–18276. https://doi.org/10.1021/jacs.0c09400
29. Davies DL, Donald SMA, Macgregor SA (2005) Computational study of the mechanism of cyclometalation by palladium acetate. J Am Chem Soc 127(40):13754–13755. https://doi.org/10.1021/ja052047w
30. García-Cuadrado D, Braga AAC, Maseras F, Echavarren AM, (2006) Proton abstraction mechanism for the palladium-catalyzed intramolecular arylation. J Am Chem Soc 128(4):1066–1067. https://doi.org/10.1021/ja056165v
31. García-Cuadrado D, de Mendoza P, Braga AAC, Maseras F, Echavarren AM, (2007) Proton-abstraction mechanism in the palladium-catalyzed intramolecular arylation: substituent effects. J Am Chem Soc 129(21):6880–6886. https://doi.org/10.1021/ja071034a
32. Gorelsky SI, Lapointe D, Fagnou K (2008) Analysis of the concerted metalation-deprotonation mechanism in palladium-catalyzed direct arylation across a broad range of aromatic substrates. J Am Chem Soc 130(33):10848–10849. https://doi.org/10.1021/ja802533u
33. Lafrance M, Rowley CN, Woo TK, Fagnou K (2006) Catalytic intermolecular direct arylation of perfluorobenzenes. J Am Chem Soc 128(27):8754–8756. https://doi.org/10.1021/ja062509l
34. Lafrance M, Gorelsky SI, Fagnou K (2007) High-yielding palladium-catalyzed intramolecular alkane arylation: reaction development and mechanistic studies. J Am Chem Soc 129(47):14570–14571. https://doi.org/10.1021/ja076588s
35. Balcells D, Clot E, Eisenstein O (2010) C—H bond activation in transition metal species from a computational perspective. Chem Rev 110(2):749–823. https://doi.org/10.1021/cr900315k
36. Cembellín S, Dalton T, Pinkert T, Schäfers F, Glorius F, (2020) Highly selective synthesis of 1,3-enynes, pyrroles, and furans by manganese(I)-catalyzed C-H activation. ACS Catal 10(1):197–202. https://doi.org/10.1021/acscatal.9b03965
37. Rogge T, Oliveira JCA, Kuniyil R, Hu L, Ackermann L (2020) Reactivity-controlling factors in carboxylate-assisted C-H activation under 4d and 3d transition metal catalysis. ACS Catal 10(18):10551–10558. https://doi.org/10.1021/acscatal.0c02808
38. Yang Q, Wu C, Zhou J, He G, Liu H, Zhou Y (2019) Highly selective C-H bond activation of N-arylbenzimidamide and divergent couplings with diazophosphonate compounds: a catalyst-controlled selective synthetic strategy for 3-phosphorylindoles and 4-phosphorylisoquinolines. Org Chem Front 6(3):393–398. https://doi.org/10.1039/C8QO01148F
39. Ma W, Weng Z, Rogge T, Gu L, Lin J, Peng A, Luo X, Gou X, Ackermann L (2018) Ruthenium(II)-catalyzed C-H chalcogenation of anilides. Adv Synth Catal 360(4):704–710. https://doi.org/10.1002/adsc.201701147
40. Lu Q, Mondal S, Cembellín S, Glorius F, (2018) MnI/AgI relay catalysis: traceless diazo-assisted C(sp2)-H/C(sp3)-H coupling to β-(hetero)aryl/alkenyl ketones. Angew Chem Int Ed 57(33):10732–10736. https://doi.org/10.1002/anie.201803384
41. Mei R, Zhang SK, Ackermann L (2017) Ruthenium(II)-catalyzed C-H alkynylation of weakly coordinating benzoic acids. Org Lett 19(12):3171–3174. https://doi.org/10.1021/acs.orglett.7b01294
42. Colletto C, Islam S, Juliá-Hernández F, Larrosa I (2016) Room-temperature direct β-arylation of thiophenes and benzo[b]thiophenes and kinetic evidence for a heck-type pathway. J Am Chem Soc 138(5):1677–1683. https://doi.org/10.1021/jacs.5b12242
43. Li J, Ackermann L (2015) Cobalt(III)-catalyzed aryl and alkenyl C-H aminocarbonylation with isocyanates and acyl azides. Angew Chem Int Ed Engl 54(29):8551–8554. https://doi.org/10.1002/anie.201501926
44. Yu DG, Gensch T, de Azambuja F, Vásquez-Céspedes S, Glorius F (2014) Co(III)-catalyzed C-H activation/formal SN-type reactions: selective and efficient cyanation, halogenation, and allylation. J Am Chem Soc 136(51):17722–17725. https://doi.org/10.1021/ja511011m
45. Engle KM, Wang DH, Yu JQ (2010) Ligand-accelerated C-H activation reactions: evidence for a switch of mechanism. J Am Chem Soc 132(40):14137–14151. https://doi.org/10.1021/ja105044s
46. Naksomboon K, Poater J, Bickelhaupt FM, Fernández-Ibáñez MA (2019) Para-selective C-H olefination of aniline derivatives via Pd/S. O-Ligand Catalysis. J Am Chem Soc 141(16):6719–6725. https://doi.org/10.1021/jacs.9b01908
47. Wang L, Carrow BP (2019) Oligothiophene synthesis by a general C-H activation mechanism: electrophilic concerted metalation-deprotonation (eCMD). ACS Catal 9(8):6821–6836. https://doi.org/10.1021/acscatal.9b01195
48. Tan E, Quinonero O, Elena de Orbe M, Echavarren AM (2018) Broad-scope Rh-catalyzed inverse-sonogashira reaction directed

by weakly coordinating groups. ACS Catal 8(3):2166–2172. https://doi.org/10.1021/acscatal.7b04395
49. Zell D, Bursch M, Müller V, Grimme S, Ackermann L, (2017) Full selectivity control in cobalt(III)-catalyzed C-H alkylations by switching of the C-H activation mechanism. Angew Chem Int Ed 56(35):10378–10382. https://doi.org/10.1002/anie.201704196
50. Ma W, Mei R, Tenti G, Ackermann L (2014) Ruthenium(II)-catalyzed oxidative C-H alkenylations of sulfonic acids, sulfonyl chlorides and sulfonamides. Chem Eur J 20(46):15248–15251. https://doi.org/10.1002/chem.201404604
51. Frisch MJ, Trucks GW, Schlegel HB, Scuseria GE, Robb MA, Cheeseman JR, Scalmani G, Barone V, Petersson GA, Nakatsuji H, Li X, Caricato M, Marenich AV, Bloino J, Janesko BG, Gomperts R, Mennucci B, Hratchian HP, Ortiz JV, Izmaylov AF, Sonnenberg JL, Williams-Young D, Ding F, Lipparini F, Egidi F, Goings J, Peng B, Petrone A, Henderson T, Ranasinghe D, Zakrzewski VG, Gao J, Rega N, Zheng G, Liang W, Hada M, Ehara M, Toyota K, Fukuda R, Hasegawa J, Ishida M, Nakajima T, Honda Y, Kitao O, Nakai H, Vreven T, Throssell K, Montgomery JAJ, Peralta JE, Ogliaro F, Bearpark MJ, Heyd JJ, Brothers EN, Kudin K, Staroverov VN, Keith TA, Kobayashi R, Normand J, Raghavachari K, Rendell AP, Burant JC, Iyengar SS, Tomasi J, Cossi M, Millam JM, Klene M, Adamo C, Cammi R, Ochterski JW, Martin RL, Morokuma K, Farkas O, Foresman JB, Fox DJ (2016) Gaussian 16, revision c. 01
52. Zhao Y, Truhlar DG (2006) A new local density functional for main-group thermochemistry, transition metal bonding, thermochemical kinetics, and noncovalent interactions. J Chem Phys 125(19):194101. https://doi.org/10.1063/1.2370993
53. Weigend F, Ahlrichs R (2005) Balanced basis sets of split valence, triple zeta valence and quadruple zeta valence quality for H to Rn: design and assessment of accuracy. Phys Chem Chem Phys 7(18):3297–3305. https://doi.org/10.1039/B508541A
54. Weigend F (2006) Accurate coulomb-fitting basis sets for H to Rn. Phys Chem Chem Phys 8(9):1057–1065. https://doi.org/10.1039/B515623H
55. Gonzalez C, Schlegel HB (1989) An improved algorithm for reaction path following. J Chem Phys 90(4):2154–2161. https://doi.org/10.1063/1.456010
56. Marenich AV, Cramer CJ, Truhlar DG (2009) Universal solvation model based on solute electron density and on a continuum model of the solvent defined by the bulk dielectric constant and atomic surface tensions. J Phys Chem B 113(18):6378–6396. https://doi.org/10.1021/jp810292n
57. Wiberg KB (1968) Application of the pople-santry-segal CNDO method to the cyclopropylcarbinyl and cyclobutyl cation and to bicyclobutane. Tetrahedron 24(3):1083–1096. https://doi.org/10.1016/0040-4020(68)88057-3
58. Reed AE, Curtiss LA, Weinhold F (1988) Intermolecular interactions from a natural bond orbital, donor-acceptor viewpoint. Chem Rev 88(6):899–926. https://doi.org/10.1021/cr00088a005
59. Cheng GJ, Yang YF, Liu P, Chen P, Sun TY, Li G, Zhang X, Houk KN, Yu JQ, Wu YD (2014) Role of N-acyl amino acid ligands in Pd(II)-catalyzed remote C-H activation of tethered arenes. J Am Chem Soc 136(3):894–897. https://doi.org/10.1021/ja411683n
60. Kozuch S, Shaik S (2006) A combined kinetic-quantum mechanical model for assessment of catalytic cycles: application to cross-coupling and heck reactions. J Am Chem Soc 128(10):3355–3365. https://doi.org/10.1021/ja0559146
61. Park CH, Ryabova V, Seregin IV, Sromek AW, Gevorgyan V (2004) Palladium-catalyzed arylation and heteroarylation of indolizines. Org Lett 6(7):1159–1162. https://doi.org/10.1021/ol049866q
62. Li L, Brennessel WW, Jones WD (2009) C-H activation of phenyl imines and 2-phenylpyridines with [Cp*MCl2]2 (M = Ir, Rh): regioselectivity, kinetics, and mechanism. Organometallics 28(12):3492–3500. https://doi.org/10.1021/om9000742
63. Pivsa-Art S, Satoh T, Kawamura Y, Miura M, Nomura M (1998) Palladium-catalyzed arylation of azole compounds with aryl halides in the presence of alkali metal carbonates and the use of copper iodide in the reaction. Bull Chem Soc Jpn 71(2):467–473. https://doi.org/10.1246/bcsj.71.467
64. Gorelsky SI, Lapointe D, Fagnou K (2012) Analysis of the palladium-catalyzed (aromatic)C-H bond metalation-deprotonation mechanism spanning the entire spectrum of arenes. J Org Chem 77(1):658–668. https://doi.org/10.1021/jo202342q
65. Jencks WP (1972) General acid-base catalysis of complex reactions in water. Chem Rev 72(6):705–718. https://doi.org/10.1021/cr60280a004
66. O'Ferrall RAM (1970) Relationships between E2 and E1cB mechanisms of β-elimination. J Chem Soc B 274–277. https://doi.org/10.1039/J29700000274